

A COUPLED CONTINUOUS-DISCONTINUOUS APPROACH TO CONCRETE ELEMENTS

J. BOBIŃSKI* AND J. TEJCHMAN†

* Gdansk University of Technology
Narutowicza 11/12, 80-233 Gdansk, Poland
e-mail: bobin@pg.gda.pl, www.pg.gda.pl

† Gdansk University of Technology
Narutowicza 11/12, 80-233 Gdansk, Poland
e-mail: tejchmk@pg.gda.pl, www.pg.gda.pl

Key words: Concrete, Crack, Strain localisation, Non-local plasticity, Extended Finite Element Model (XFEM)

Abstract: The paper deals with numerical simulations of fracture in concrete using a continuous, discontinuous and coupled continuous-discontinuous constitutive model. In a continuum approach, cracks were treated in a smeared sense with an elasto-plastic constitutive law with Rankine criterion. To ensure mesh-insensitive results, an integral non-local theory was applied. Alternatively, cracks were described as displacement jumps using the eXtended Finite Element Method (XFEM). A coupled model of these two formulations was also proposed. Some benchmark tests were performed.

1 INTRODUCTION

Modelling of quasi-brittle materials like concrete is demanding task due to the presence of material fracture. At the beginning of loading, a region with several micro-cracks is formed. Later these micro-cracks create discrete macro-cracks. There exist two basic approaches to simulate cracks in solid bodies. The first idea is based on a continuum description. The material can be described using e.g. elasto-plastic, damage mechanics or coupled constitutive laws. These formulations include softening, so they have to be equipped with a characteristic length of microstructure to preserve the well-posedness of the boundary value problem. It can be achieved by means of e.g. micro-polar, non-local or gradient theories. Alternatively, a crack can be regarded as a discrete macro-crack with a displacement jump (by omitting a micro-crack phase). The oldest solutions used interface elements

defined along element edges. The modern ones allow for considering cracks in the interior of finite elements using embedded discontinuities or XFEM (eXtended Finite Element Method) [1] based on a concept of the partition of unity. Continuum constitutive laws are more realistic in describing strain localization phenomena, but they cannot properly capture the crack formation and propagation. Discontinuous models, on the other hand, can handle macro-cracks, but they cannot describe localized zones. A combination of a continuous and discontinuous approach enables to capture a full fracture process. Such coupling can be done in several ways, e.g. the latest approaches combine XFEM with implicit gradient [2] or integral-nonlocal [3] isotropic damage models. Wells et al. [4] combined XFEM with the Perzyna viscoplastic model.

The paper presents FE results obtained with a continuous elasto-plastic model and non-

local softening and a discontinuous XFEM approach. A coupling formulation between these two models was also proposed.

2 CONTINUUM CONSTITUTIVE MODEL

An elasto-plastic constitutive law with standard Rankine yield criterion was used

$$f = \sigma_{\max} - \sigma_t(\kappa), \quad (1)$$

where σ_{\max} – maximum principal stress, σ_t – tensile yield stress and κ – hardening/softening parameter. The associated flow rule was assumed. To define softening under tension, a curve proposed by Hordijk [5] was applied

$$\sigma_t(\kappa) = f_t \left(\left(1 + (A_1 \kappa)^3 \right) \exp(A_2 \kappa) - A_3 \frac{\kappa}{\kappa_u} \right) \quad (2)$$

with κ_u – ultimate value of the softening parameter at the non-zero yield stress and constants A_1, A_2 and A_3 are defined as

$$A_1 = \frac{c_1}{\kappa_u} \quad A_2 = -\frac{c_2}{\kappa_u} \quad A_3 = \left(1 + c_1^3 \right) \exp(-c_2) \quad (3)$$

with the coefficients $c_1=3.0$ and $c_2=6.93$.

To obtain mesh-objective results within continuum constitutive models including material softening, an integral non-local theory was used as a regularisation technique [6]. In plasticity, rates of the softening parameter $d\kappa$ were treated non-locally according to Brinkgreve [7]

$$d\bar{\kappa}(\mathbf{x}) = (1-m)d\kappa(\mathbf{x}) + md\hat{\kappa}(\mathbf{x}) \quad (4)$$

with

$$d\hat{\kappa}(\mathbf{x}) = \frac{\int_V \alpha_0(\|\mathbf{x} - \boldsymbol{\xi}\|) d\kappa(\boldsymbol{\xi}) d\boldsymbol{\xi}}{\int_V \alpha_0(\|\mathbf{x} - \boldsymbol{\xi}\|) d\boldsymbol{\xi}}, \quad (5)$$

where \mathbf{x} - coordinates of considered (actual) point, $\boldsymbol{\xi}$ – coordinates of the surrounding points, m – non-locality parameter (it should be greater than 1). The weighting function (Gauss distribution) was defined as

$$\alpha_0(r) = \frac{1}{l\sqrt{\pi}} e^{-\left(\frac{r}{l}\right)^2}, \quad (6)$$

where r – distance between points, l – characteristic length of the microstructure.

In FE-simulations an approximated method was used to evaluate non-local quantities. In the given integration point, the influence of its neighbours was determined using the values from the previous iteration. It enabled us to simplify calculations and to preserve locality of plasticity algorithms.

3 DISCONTINUOUS APPROACH

To describe displacement jumps in continuum, the eXtended Finite Element Method (XFEM) was chosen. It is based on the Partition of Unity (PUM) and it allows for defining cracks across finite elements. It is achieved by adding locally extra known terms to a standard FE displacement approximation.

The formulation used follows (with some slight modification and improvements) the general idea presented by Wells and Sluys [8] based on the so-called shifted-basis enrichment [9] to describe a displacement field with discontinuous jumps. In the initial continuum body, a linear elastic constitutive law was assumed. A new crack could be activated or an existing crack could propagate, if the standard Rankine's criterion ($\sigma_{\max} > f_t$) was fulfilled at least in one point of the element at the front of the crack tip. A new segment was added to cracks with a new crack tip located at the element edge.

To find a direction of the crack propagation, the direction of the crack extension was assumed to be perpendicular to the direction of the maximum principal stress. To smoothen the stress field around the crack tip, the average stresses σ^* was used for determining the crack direction according to Wells and Sluys [8]

$$\sigma^* = \int_V \sigma w dV, \quad (7)$$

where V - semicircle domain at the front of the crack tip, w – weight function assumed as

$$w(r) = \frac{1}{(2\pi)^{3/2} l_{av}^3} \exp\left(-\frac{r^2}{2l_{av}^2}\right) \quad (8)$$

with l_{av} as the averaging length related to the size of finite elements (not equivalent with a characteristic length of microstructure). In the research literature, more advanced algorithms can be found. Oliver et al. [10] formulated so-called global tracking algorithm. The propagation directions of all cracks were determined globally by solving a stationary anisotropic heat conduction problem. Moës and Belytschko [11] assumed that cohesive tractions had no influence on the crack propagation direction and used the maximum circumferential stress criterion from Linear Elastic Fracture Mechanics (LEFM).

After Wells and Sluys [8], the following format of the loading function within discrete cohesive laws was assumed

$$w(r) = \frac{1}{(2\pi)^{3/2} l_{av}^3} \exp\left(-\frac{r^2}{2l_{av}^2}\right) \quad (9)$$

with the history parameter κ equal to the maximum value of the displacement jump $[[u_n]]$ achieved during loading. The softening of the normal component of the traction vector was described using either an exponential relationship

$$t_n = D_f f_t \exp\left(-\frac{f_t \kappa}{G_f}\right) \quad (10)$$

or a linear one

$$t_n = D_f f_t \left(1 - \frac{f_t \kappa}{2G_f}\right), \quad (11)$$

where G_f – fracture energy, D_f – correction term defined as

$$D_f = 1 - \exp\left(-d_f \frac{\kappa}{\kappa_u}\right) \quad (12)$$

with the drop factor d_f [12]. This factor improves the convergence under tensile-compressive load changes. With increasing value of d_f , the term D_f approaches 1. During unloading, the secant stiffness was used with a return to the origin (damage format). In a compressive regime, the penalty stiffness in the normal direction was used (depending upon the drop factor d_f). In the tangent

direction, a linear relationship between a displacement jump and traction was defined with the stiffness T_S .

4 COUPLED NUMERICAL APPROACH

A coupled model enables to simulate both the creation of localised zones of deformation and the evolution of discrete cracks. During the first phase, the elasto-plastic constitutive law described in Section 2 was used. If the specified value of the softening parameter κ was exceeded in any of integration points in the element at the front of the crack tip, the formulation switched to a cracked element. A new crack segment was introduced. The direction of a discrete crack propagation \mathbf{p} was determined by (similar as in [4])

$$\mathbf{p} = \int_V \kappa(\xi) w(\xi) \bar{\mathbf{p}}(\xi) dV \quad (13)$$

where $\bar{\mathbf{p}}$ – normalized direction from crack tip to the point, w – weight function defined in Eqn. (9). An introduction of a crack segment preserved the stress equilibrium. Therefore cohesive discrete material behaviour was modified to take into account the initial displacement jumps $[[u_n^{init}]]$ and $[[u_s^{init}]]$. These values were determined on the basis on the known tractions t_n^{init} and t_s^{init} at the moment of a crack creation and the defined relationships in a normal and tangential direction. In other words, XFEM softening in normal direction started not from the value f_t (peak) but from the smaller value t_n^{init} . The initial displacement $[[u_n^{init}]]$ was also added to the softening parameter κ .

The addition of a new crack segment introduced also a new barrier in non-local interactions (the points lying at the opposite sides of a crack might not see each other in non-local summations causing the so-called “shading effect”). This operation is equivalent to new boundary conditions in a coupled gradient damage and XFEM model [2]. This assumption is correct for the case when the transition from a continuous to discontinuous crack description of takes place at very small

values of t_n^{init} . If the transition point is defined, e.g. at the level of $0.5f_t$, this operation seems however to be questionable.

5 EXPERIMENTS BY NOORU-MOHAMED

5.1 Problem

As a representative benchmark problem, a double-edge notched (DEN) concrete specimen under combined shear and tension was analysed (so-called the Nooru-Mohammed test [13]). The length and height of the element were 200 mm, and the thickness was 50 mm (Fig. 1). Two notches with dimensions of $25 \times 5 \text{ mm}^2$ were located in the middle of the vertical edges. During the analysed load scenario in calculations, the shear force P_s was applied until it reached a specified value, while the horizontal edges were free. Then the shear force remained constant and the vertical tensile displacement was prescribed. In the experiment, two curved cracks with an inclination depending upon the shear force were obtained (at the small value of P_s – the cracks were almost horizontal, at the large value of P_s – the cracks were strongly curved), Fig. 2. Apart from a comparison of force – displacement diagrams, the distance d defined as the maximum distance between a horizontal line between notches and all points lying on crack curves was calculated as the indicator of a realistic numerical crack reproduction. In the experiments, it was calculated as an average value of 4 cracks and it was equal to 1.6 cm, 3.6 cm and 5.3 cm at the shear force 5 kN, 10 kN and 27.5 kN, respectively. In all simulations, the following elastic constants were assumed in calculations: Young’s modulus $E=32.8 \text{ GPa}$ and Poisson’s ratio $\nu=0.2$.

5.2 FE results within elasto-plasticity

First, the FE simulations with the enhanced standard elasto-plastic Rankine model were performed. The tensile strength was $f_t=2.4 \text{ MPa}$ and the parameter $\kappa_i=0.02$ to fit the experimental force – displacement curves. The characteristic length was equal to $l=2 \text{ mm}$

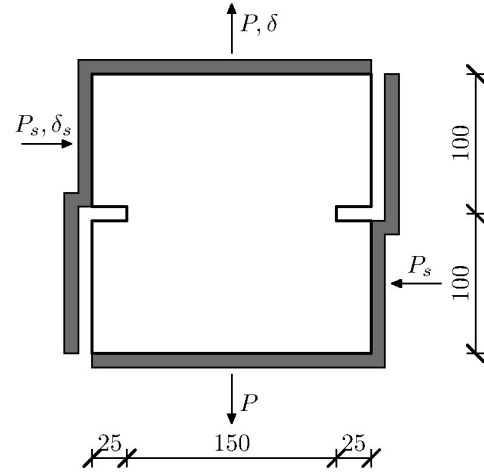


Figure 1: Nooru-Mohamed test [13]: geometry and boundary conditions.



Figure 2: Nooru-Mohamed test [13]: experimental crack pattern at $P_s=10 \text{ kN}$.

and the non-locality parameter was $m=2$. The FE-mesh included 8585 quadrilateral elements. The obtained FE results are presented in Figs. 3 and 4 (the cracks are shown via the contours of the softening parameter κ). In the case of the force-displacement diagrams, a very good agreement with the experimental data was obtained when the shear forces was 5 kN and 10 kN. A significant discrepancy was obtained at the maximum shear force of $P_s=24.5 \text{ kN}$, although a compressive tendency under tensile loading was properly simulated.

A crack propagation was satisfactorily reproduced in FE analyses. The distance d was equal to 2.4 cm, 3.6 cm and 5.6 cm at the small, medium and large shear force, respectively. The only drawback of calculated cracks was the fact that they were too straight at the deformation beginning.

It should be noted that similar satisfactory results were also obtained using an isotropic

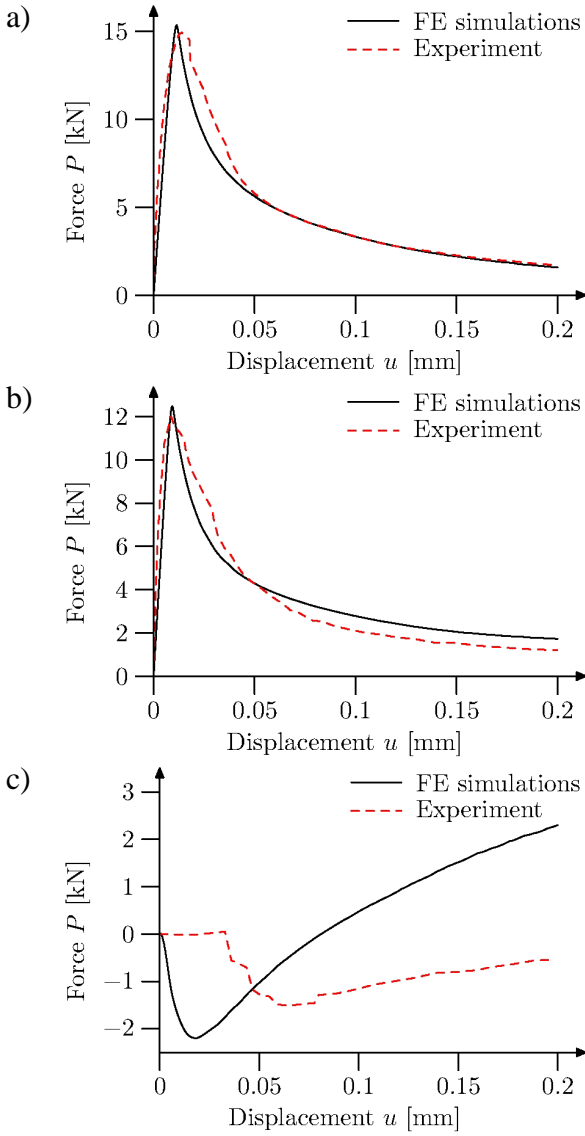


Figure 3: Force-displacement curves in Nooru-Mohamed test and in simulations using elasto-plastic model at shear force P_s equal to 5 kN (a), 10 kN (b) and 24.5 kN (c).

damage constitutive law with non-local enrichment [14].

5.3. XFEM results

The following material parameters were assumed in simulations: $f_t=2.3$ MPa and $G_f=75$ N/m to fit the experimental force-displacement curve. The averaging length was taken as $l_{av}=7.5$ mm. To avoid sudden changes of a crack direction, a limit of the maximum direction change of 10° was imposed. A mesh included 6520 3-node triangular elements. Figures 5 and 6 present the numerical results.

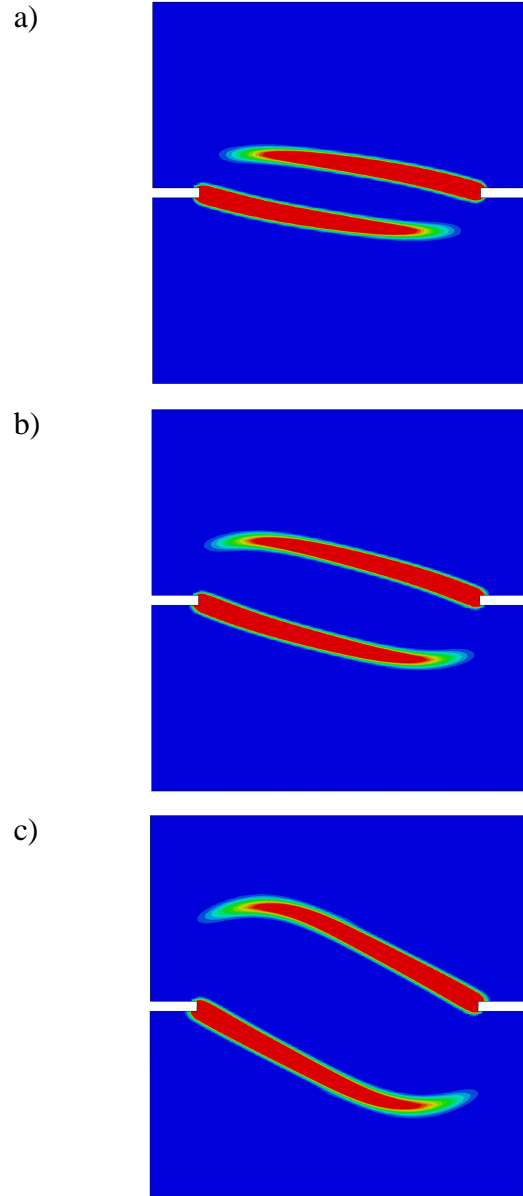


Figure 4: Smearred crack patterns in Nooru-Mohamed test and in simulations using elasto-plastic model at shear force P_s equal to 5 kN (a), 10 kN (b) and 24.5 kN (c).

A very good agreement for the force-displacement curves at the shear forces $P_s=5$ kN and $P_s=10$ kN was achieved. For the maximum shear force equal to $P_s=25$ kN (less than in the experiment), large discrepancies were observed (although a compressive nature of the vertical force under tension was properly reproduced). In all tests, two curved cracks were calculated with increasing curvature with respect to the increasing shear force. These cracks were too curved. The

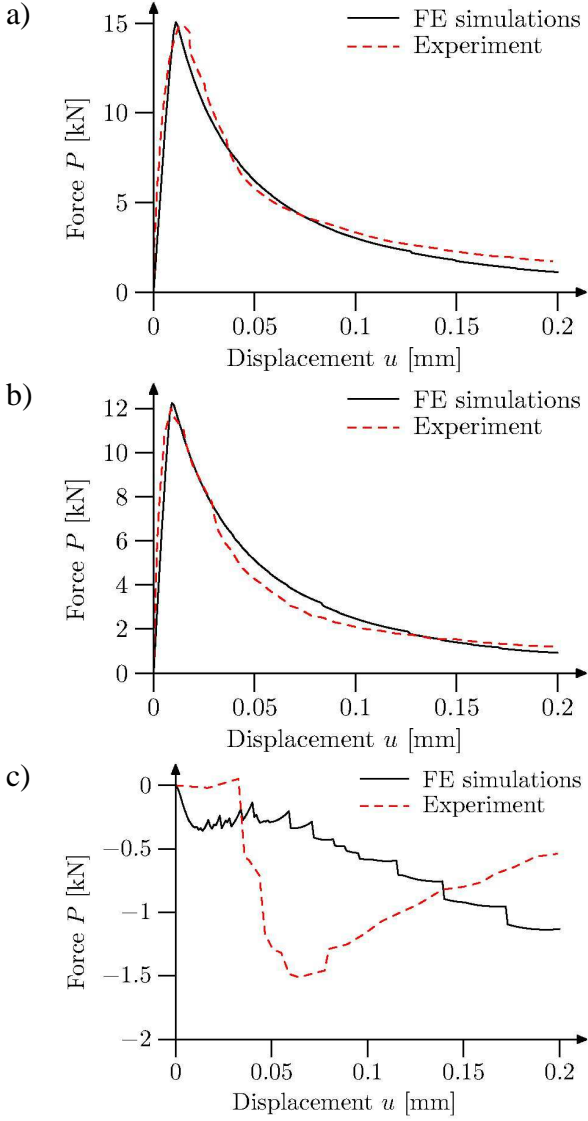


Figure 5: Force-displacement curves in Nooru-Mohamed test and in simulations using XFEM at shear force P_s equal to 5 kN (a), 10 kN (b) and 24.5 kN (c).

distance d was equal to 3.0 cm, 4.5 cm and 7.5. cm at the shear force equal to 5 kN, 10 kN and 25 kN, respectively. Thus, the existing algorithm for a crack propagation direction requires improvements to better match the experimental results. The application of other formulations did not improve the results.

Table 1 shows the distances d calculated during simulations of the Nooru-Mohamed test using XFEM performed by other researches. It can be seen that usually the problem with $P_s=10$ kN was investigated only. The obtained distances d are more close to the maximum value (not to the average one). In general,

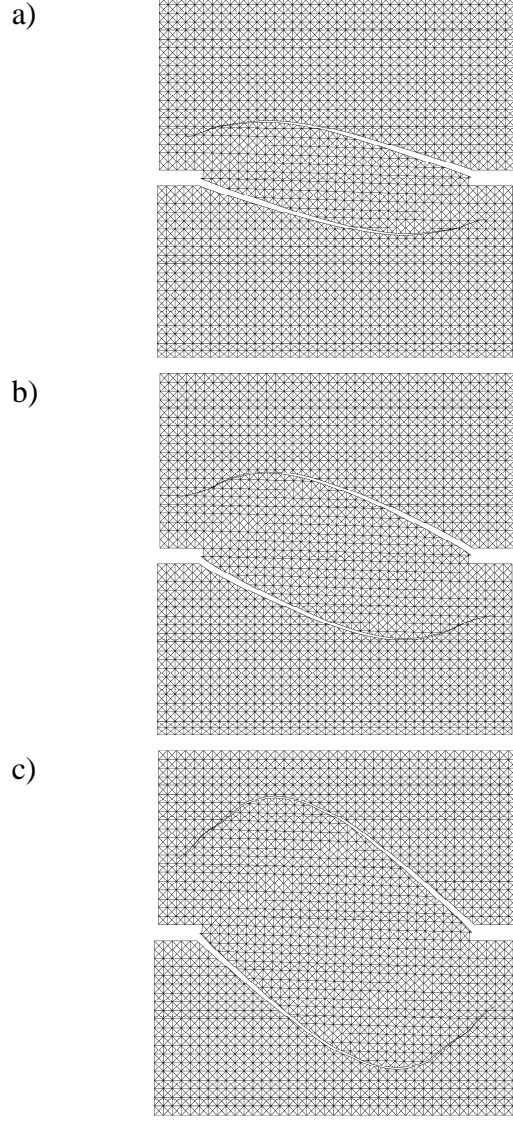


Figure 6: Discrete crack patterns in Nooru-Mohamed test and in simulations using XFEM at shear force P_s equal to 5 kN (a), 10 kN (b) and 24.5 kN (c).

Table 1: Calculated distances d (in cm) when simulating Nooru-Mohamed test at different shear force P_s (5 kN, 10 kN and 27.5 kN)

Author	5 kN	10 kN	27.5 kN
[12]		4.3	
[15]		4.1	
[16]		4.6	
[17]	3.0	4.5	7.6
[18]	1.8	2.7	

these results confirm our conclusions. Even the use of Global Tracking Algorithm [10] does not improve the crack pattern [17].

6 COUPLED APPROACH EXAMPLE

As the preliminary example, uniaxial tension was numerically analysed. A set of diagonally crossed 3-node elements was defined with 40 finite elements. The left edge was fixed while the horizontal displacement $\Delta u=0.1$ mm was applied at the right edge. The Young's modulus was equal to 30 GPa and the Poisson's ratio was taken as 0. In a continuum model, the tensile strength was $f_t=2.4$ MPa and the ultimate softening parameter $\kappa_u=0.002$. A linear softening curve was assumed. The characteristic length was $l=1$ cm and the non-locality parameter $m=2$. To induce a localized zone, the tensile strength was reduced in a central zone down to 2.3 MPa. For the XFEM model, linear softening was also assumed with the fracture energy $G_f=87$ N/m. This value was so scaled in order to obtain the almost identical force-displacement diagram in a pure continuous or discontinuous approach.

Figure 7 presents the force displacement curves at the different transition softening parameters κ_t . Despite the fact that some fluctuations are observed near the transition point, all curves are very similar.

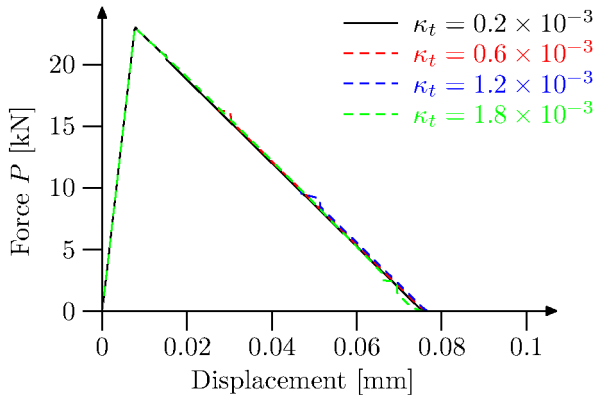


Figure 7: Calculated force-displacement curves with coupled approach and different values of κ_t .

7 CONCLUDING REMARKS

The FE simulations show that both a continuous and a discontinuous approach are able to simulate curved cracks in concrete elements. A very good agreement was obtained between numerical and experimental force-displacement curves at the shear forces of 5 kN and 10 kN. For the experimental

maximum shear force, some differences were observed but a compressive nature of the vertical force response was reproduced. All constitutive models properly reproduced the experimental crack pattern in the experiment by Nooru-Mohammed. When analysing the crack trajectory results, a continuous approach was more realistic than XFEM.

Currently, some verification procedures and improvements of the defined coupled model are performed using the isotropic damage constitutive law with non-local softening and XFEM is under development. The choice of a transition point between continuous and discontinuous displacements will be numerically analysed and FE results will be directly compared with experimental results of measured displacements on the surface of notched concrete beams under 3-point bending using a digital correlation image (DIC) technique [19].

ACKNOWLEDGMENTS

Scientific work has been carried out as a part of the Project: “Innovative resources and effective methods of safety improvement and durability of buildings and transport infrastructure in the sustainable development” financed by the European Union (POIG.01.01.02-10-106/09-01).

The FE calculations were carried out at the Academic Computer Center in Gdańsk.

REFERENCES

- [1] Moës, N., Dolbow, J. and Belytschko, T., 1999. A finite element method for crack growth without remeshing. *Int. J. Num. Meth. Engng.* **46**:131-150.
- [2] Simone, A., Wells, G.N. and Sluys, L.J., 2003. From continuous to discontinuous failure in a gradient-enhanced continuum damage model. *Comput. Meth. Appl. Mech. Eng.* **192**:4581-4607.
- [3] C. Comi, C., Mariani, S. and Perego, U., 2007. An extended FE strategy for transition from continuum damage to mode I cohesive crack propagation. *Int. J.*

- Numer. Anal. Meth. Geomech.* **31**:213-238.
- [4] Wells, G.N., Sluys, L.J. and de Borst, R., 2002. Simulating the propagation of displacement discontinuities. *Int. J. Num. Meth. Engng.* **53**:1235-1256.
- [5] Hordijk D.A., 1991. *Local approach to fatigue of concrete*, PhD Thesis, TU Delft.
- [6] Tejchman J. and Bobiński J., 2012. *Continuous and discontinuous modeling of fracture in concrete using FEM*, Springer, Berlin-Heidelberg.
- [7] Brinkgreve R., 1994. *Geomaterial models and numerical analysis of softening*. PhD Thesis, TU Delft.
- [8] Wells G.N. and Sluys L.J., 2011. A new method for modelling cohesive cracks using finite elements. *Int. J. Num. Meth. Engng.* **50**: 2667–2682.
- [9] Zi, G. and Belytschko, T., 2003. New crack-tip elements for XFEM and applications to cohesive cracks. *Int. J. Num. Meth. Engng.* **57**:2221-2240.
- [10] Oliver, J., Huespe, A.E., Samaniego, E. and Chaves, E.W., 2004. Continuum approach to the numerical simulation of material failure in concrete. *Int. J. Numer. Anal. Meth. Geomech.* **28**: 609-632.
- [11] Moës, N. and Belytschko, T., 2002. Extended finite element method for cohesive crack growth. *Eng. Fract. Mech.* **69**:813-833.
- [12] Cox, J.V., 2009. An extended finite element method with analytical enrichment for cohesive crack modelling. *Int. J. Num. Meth. Engng.* **78**:48-83.
- [13] Nooru-Mohamed M.B., 1992. *Mixed mode fracture of concrete: an experimental research*. PhD Thesis, TU Delft.
- [14] Bobiński, J. and Tejchman J., 2012. Investigations of different crack propagation criteria in simulations of concrete behavior using XFEM. *Eccomas Congress, Vienna, Austria*.
- [15] Dumstorff, P. and Meschke, G., 2007. Crack propagation criteria in the framework of X-FEM-based structural analyses. *Int. J. Numer. Anal. Meth. Geomech.* **31**:239-259.
- [16] Gasser, T.C., and Holzapfel, G.A., 2006. 3D Crack propagation in unreinforced concrete. A two-step algorithm for tracking 3D crack paths. *Comput. Meth. Appl. Mech. Eng.* **195**:5198-5219.
- [17] Meschke, G. and Dumstorff, P., 2007. *Energy-based modeling of cohesive and cohesionless cracks via X-FEM*. *Comput. Meth. Appl. Mech. Eng.* **196**:2338-2357.
- [18] Unger, J.F., Eckardt, S. and Könke, C., 2007. Modelling of cohesive crack growth in concrete structures with the extended finite element method. *Comput. Meth. Appl. Mech. Eng.* **196**:4087-4100.
- [19] Skarżyński, Ł., Syroka, E. and Tejchman, J., 2011. Measurements and calculations of the width of the fracture process zones on the surface of notched concrete beams, *Strain*, **47**:e319-e332.